PHYSICAL REVIEW B VOLUME 51, NUMBER 2 1 JANUARY 1995-II

Flux pinning and critical current in layered type-II superconductors in parallel magnetic fields

Vesna Prokić
Department of Physics, University of Belgrade, P.O. Box 368, 11001 Belgrade, Yugoslavia

Dragomir Davidović
Institute of Physics, P.O. Box 57, 11001 Belgrade, Yugoslavia
and Department of Physics and Astronomy, The Johns Hopkins University, Bloomberg Center, Baltimore, Maryland 21218

Ljiljana Dobrosavljević-Grujić
Institute of Physics, P.O. Box 57, 11001 Belgrade, Yugoslavia
(Received 3 August 1994)

We have shown, within the Ginzburg-Landau theory, that the interaction between vortices and normal-metal layers in high-T_c superconductor–normal-metal superlattices can cause high critical-current densities j_c. The interaction is primarily magnetic, except at very low temperatures T, where the core interaction is dominant. For a lattice of vortices commensurate with an array of normal-metal layers in a parallel magnetic field **H**, strong magnetic pinning is obtained, with a nonmonotonic critical-current dependence on H, and with j_c of the order of 10^7-10^8 A/cm^2.

I. INTRODUCTION

Soon after the discovery of the layered high-temperature (HTC) superconductors, a mechanism of vortex pinning was proposed:[1,2] intrinsic pinning of vortices due to their interaction with the layered structure. When the magnetic field and the transport current are perpendicular to each other and lie in the plane of the layers, this pinning mechanism may be the dominant one, provided that the vortex lattice is commensurate with the interlayer spacing. Recently, experimental observations of intrinsic pinning were reported.[3,4] One possible explanation for intrinsic pinning is the variation of the condensation energy when the vortex core crosses the layer, resulting from the modulation of the superconducting order parameter. This is known as *core pinning*. When the vortex lattice is incommensurate with the interlayer spacing, the average depinning current vanishes. Strong pinning and high critical current are expected in commensurate vortex lattices consisting of chains of vortices centered in regions between the superconducting layers. The distance between adjacent vortices is then an integer multiple of the interlayer spacing.[2]

Historically, intrinsic pinning and commensurability effects were observed not only in conventional layered superconductors, such as $NbSe_2$,[5] but also in artificially prepared superconductors with a periodic distribution of inhomogeneities. Examples of the latter include Al films with periodically modulated thickness[6] and Pb/Bi alloys with a periodic modulation of Bi concentration.[7] Much stronger intrinsic pinning is obtained in periodic structure consisting of two different materials, such as PbIn/SnIn superlattices,[8] and Nb/NbZr superlattices.[9] In such systems the intrinsic pinning can result not only from variations in the condensation energy, but also from variations in the electromagnetic energy. When the vortex is in an asymmetric position with respect to the pinning center, and the pinning center is a normal or weakly superconducting layer, the local field and supercurrent distribution become asymmetric as well, resulting in a force pushing the vortex back to the center. We expect that this *magnetic pinning* can also be strong in artificial HTC superconductor–normal-metal superlattices, and that in layered HTC superconductors it can contribute to the intrinsic pinning. This is because in the limit of very large $\kappa=\lambda/\xi$ the vortex energy is essentially the magnetic energy, and it can be significantly changed by the order-parameter modulation. In effect, this modulation strongly perturbs the supercurrent distribution around vortices, and that is the main contribution to the vortex energy. Such an enhancement of magnetic pinning is valid only for low applied magnetic field. If the magnetic field is large, the distance between vortices is small, and the field is practically uniform. Then we expect that the core pinning is dominant. The magnetic pinning of a vortex system in a layered superconductor is the strongest in commensurate configurations, where the pinning centers act synchronously,[10] and the field is close to "matching" fields at which the nondeformed hexagonal vortex lattice is commensurate with the periodic pinning potential. Theoretically, pinning in modulated structures was studied by Dobrosavljević[11] and by Martinoli[12] in the London limit, and by Ami and Maki[13] in the Abrikosov (high-field) limit. An extensive review of experimental and theoretical work on pinning by artificial periodic structures is presented by Lykov.[14] Recently, magnetic pinning of a single vortex parallel to a superconductor–normal-metal–superconductor ($S/N/S$) junction was studied by Davidović and Dobrosavljević-Grujić,[15] whereas intrinsic pinning in a superconductor-superconductor (S/S') superlattice was considered by Tachiki, Takahashi, and Sunaga.[16] In previous work[15]

0163-1829/95/51(2)/1270(7)/$06.00

we have shown that when the normal-metal coherence length ξ_N is small compared to the superconductor penetration depth λ_S, the magnetic pinning interaction increases rapidly with the N-layer relative thickness a_N/ξ_N. Then, since the coherence length in a normal metal is inversely proportional to T, it follows that the pinning force can be an increasing function of temperature. This behavior can produce a "stabilization" effect in the critical current.

With the aim to obtain strong magnetic pinning at a relatively high temperature, we consider a S/N superlattice with S layers consisting of a HTC superconductor, with large κ_S, and N layers of a normal metal with small coherence length, comparable to that of S. The external magnetic field $\mathbf{H}$ is assumed to be parallel to the layers, and to lie in the range $H_{c1}^N < H \sim H_{c1}^S$, where H_{c1}^N is the lower critical field for penetration in N layers, and H_{c1}^S that of bulk S. This choice of fields guarantees the stability of vortex structures commensurate with the superlattice, since for $H \gtrsim H_{c1}^N$ vortices penetrate in the form of vortex chains centered in the N layers.[15] The period of such a first-order commensurate structure is ma, where a is the superlattice period and $m=1,2,3.\ldots$ In relatively low fields, where the distance between vortices is comparable to λ_S, we expect the main first-order commensurate structure $m=1$, for which the pinning force is the largest, to be stable provided that $a \sim \lambda_S$. Such a choice of the superlattice period allows one to consider the $m=1$ configuration only. Also, in the considered range of fields the pinning strength can be regarded as field independent. A preliminary report on this research is presented in Ref. 17.

In Sec. II, we derive the expressions for vortex-lattice magnetic free energy, Gibbs energy, and pinning force using the London approximation of the Ginzburg-Landau (GL) theory for dirty metals. We work in the limit $\kappa_S \gg 1$, $\xi_N \sim \xi_S$, and $a_N \ll \lambda_S$, where κ_S, ξ_S, and λ_S are the GL parameter, coherence length, and penetration depth in the superconductor, respectively, and a_N is the N-layer thickness. The assumption of small normal-layer thickness allows an analytic solution of the London equation, similarly to the single-vortex case.[15] The condensation energy and the corresponding pinning force are calculated within GL theory, using the results of Ref. 15. The critical current is determined by the maximum of the *total, magnetic and core* pinning force from the force-balance equation. In Sec. III we present our results, i.e., dependence of the pinning force on the magnetic field, temperature, and on the parameters characteristic for the S and N layers. We show under which conditions the strong intrinsic pinning is primarily magnetic. The critical-current density $j_{cr}(H)$ exhibits typical nonmonotonic behavior, with a maximum at the corresponding "matching" field. A short discussion (Sec. IV) of the results and of the peak-effect mechanism concludes the paper.

II. PINNING ENERGY, PINNING FORCE, AND CRITICAL CURRENT

We consider the main commensurate $(m=1)$ vortex lattice, choosing the superlattice period $a \sim \lambda_S$, so that the lattice is stable in a domain of external magnetic field near H_{c1}^S. The stability domain is determined as a function of characteristics of the S and N layers and of the temperature T (see below). The external magnetic field $\mathbf{H}$ is assumed parallel to the z axis, the yz plane being parallel to the superlattice layers.

In the $m=1$ configuration the vortices are situated at the position (Fig. 1)

$$\mathbf{r}_{i,j}=(ia+c)\mathbf{e}_x+(j-\tfrac{1}{2})L\mathbf{e}_y\ , \quad i,j=0,\pm1,\pm2,\ldots \tag{1}$$

where the intrachain vortex distance L is a function of the external field H and of the vortex-lattice displacement c from the middle of the central (arbitrarily chosen) N layer. We note that in the ground state $c=0$, but to calculate the pinning force we consider the case $c\neq0$ as well. By assuming both S and N metals are dirty and working in the high-T_c limit, $(\kappa_S \gg 1)$, we calculate the magnetic energy density of the system of vortices (in physical units) in the modified London approximation,[18,19]

$$E_{\rm phys}^m=\frac{1}{8\pi A}\int[h^2+\lambda^2(\mathbf{r})(\nabla\times\mathbf{h})^2]d^2\mathbf{r}\ . \tag{2}$$

Here A is the area occupied by vortices, $\lambda^2(\mathbf{r})=\lambda_S^2/g^2(\mathbf{r})$ is the spatially dependent magnetic penetration depth, and $g(\mathbf{r})$ is the normalized periodic order parameter, with period a. For N layers much thinner than S layers, $a \gg a_N$, and in low fields $g(x)$ can be constructed by periodic repetition of the zero-field solution obtained in Ref. 15 for a single $S/N/S$ junction. The latter is different from 1 only in a small interval that includes the N layer and adjacent regions in S of order ξ_S,[15]

$$g(x)=\begin{cases}\tanh\left[\dfrac{b}{\sqrt{2}\xi_S}\right]\dfrac{\cosh[(x-c)/\xi_N]}{\cosh(a_N/\xi_N)}\ , & |x-c|<a_N\ ,\\[2ex] \tanh\left[\dfrac{|x-c|+b-a_N}{\sqrt{2}\xi_S}\right]\ , & |x-c|\geq a_N\ ,\end{cases} \tag{3}$$

where

$$b=\frac{\xi_S}{\sqrt{2}}\sinh^{-1}\left[\frac{\sqrt{2}\xi_N}{\xi_S}\coth\left[\frac{a_N}{\xi_N}\right]\right]\ . \tag{4}$$

In the following, we express all of the physical quantities in standard reduced units,[15] taking λ_S as the unit of length, $\sqrt{2}H_c^S$ as the unit of the magnetic field, and $(H_c^S)^2/4\pi$ as the unit of energy density. In reduced units the magnetic energy density $E_{\rm red}^m$ is given by

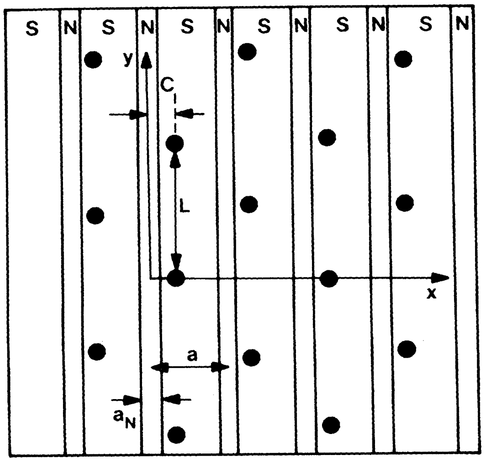

FIG. 1. The main commensurate vortex lattice $m=1$, displaced by distance c from its ground-state position.

$$E^m_{\text{red}} = \frac{1}{A}\int \left[h^2 + \frac{1}{g^2}(\nabla \times \mathbf{h})^2 \right] d^2r \ , \tag{5}$$

where $h(\mathbf{r})$ is the solution of the generalized London equation

$$h - \nabla \frac{1}{g^2} \nabla h = \frac{2\pi}{\kappa_S} \sum_{i,j} \delta(\mathbf{r} - \mathbf{r}_{ij}) \ . \tag{6}$$

Using Eq. (6), Eq. (5) can be transformed to

$$\tilde{E}^m = \frac{\kappa_S E^m_{\text{red}}}{4\pi} = \frac{1}{2A} \sum_{i,j} h(\mathbf{r}_{ij}) = \frac{N_v h(0,0)}{4A} \ , \tag{7}$$

where $h(0,0)$ is the magnetic field at the vortex at the (arbitrarily chosen) origin, generated by all other vortices in the lattice, and N_v is the number of vortices on A.

For $a_N \ll 1$, an approximate solution of Eq. (6) at a given H can be found in a manner similar to that of the single-vortex solution,[15] by noting that the order parameter $g(x)$ is different from 1 in a small interval around each defect, of thickness $\sim 1/\kappa_S$. Outside these intervals, the solution of Eq. (6) with $g(x)=1$ is asymptotically equal to the exact solution and can be determined using the boundary conditions at the N layers[15] and the symmetry requirements imposed by the periodicity of the magnetic field distribution in the vortex lattice. In this way we find $h(0,0)$ (see the Appendix), and, from Eq. (7), $\tilde{E}^m$:

$$\tilde{E}^m = \frac{\pi}{aL^2\kappa_S} \sum_{l=-\infty}^{+\infty} \frac{1+\Gamma[(Q^2-1)/Q][\sinh Qc \sinh Q(a-c)/\sinh Qa]}{\Gamma(Q^2-1)+2Q[\cosh Qa - (-1)^l]/\sinh Qa} \ , \tag{8}$$

where $Q=\sqrt{4\pi^2 l^2/L^2+1}$, and $\Gamma = \int dx (g^{-2}-1)$ is the pinning strength,

$$\Gamma = 2\sqrt{2}\left[\coth\left[\frac{b\kappa_S}{\sqrt{2}}\right] - 1\right]\frac{1}{\kappa_S} + \xi_N \sinh\left[\frac{a_N}{\xi_N}\right]\coth^2\left[\frac{b\kappa_S}{\sqrt{2}}\right] - a_N \ . \tag{9}$$

The corresponding Gibbs energy density is

$$\tilde{G}^m = \tilde{E}^m - \frac{H}{aL} \ , \tag{10}$$

and $L=L(c,H)$ is obtained from the vortex-configuration stability condition

$$\frac{\partial \tilde{G}^m}{\partial L} = 0 \ . \tag{11}$$

Here, we do not perform a rigid translation of the vortex lattice, but instead calculate the optimal intravortex distance L for each vortex-lattice displacement c.

The magnetic pinning force $\tilde{f}^m = d\tilde{G}^m/dc$ is thus given by the derivative of $\tilde{E}^m$, Eq. (8),

$$\tilde{f}^m = \frac{\pi}{aL^2\kappa_S} \times \sum_{l=-\infty}^{+\infty} \frac{\Gamma(Q^2-1)\sinh Q(a-2c)/\sinh Qa}{\Gamma(Q^2-1)+2Q[\cosh Qa - (-1)^l]/\sinh Qa} \ . \tag{12}$$

From Eq. (12) one can see that the greatest value of pinning force is obtained for the lowest allowed value of c, which we denote by c^* and which is, within the present approximation, of the order of $1/\kappa_S$. As in the single-vortex case,[15] we choose this critical value c^* so that $\tilde{E}^m(c)$ is smooth and goes linearly to $\tilde{E}^m(c=0)$ when $c<c^*$:

$$\tilde{E}^m(0) + \tilde{f}^m(c^*)c^* = \tilde{E}^m(c^*) \ . \tag{13}$$

To determine the *critical state* of the vortex system, we have to solve simultaneously Eq. (13) for the critical displacement c^* and Eq. (11) for $L(c^*)$. This is done numerically, and the divergences which appear in the sums of Eqs. (8), (12), and (13) as a consequence of the London approximation are eliminated by a cutoff of the sums at $l_{\max} = (L/2\pi)\kappa_S$.

For a given set of material parameters characterizing the system, the critical state has to be determined for each given value of temperature T and of applied magnetic field H. The results are meaningful provided that H belongs to the range of fields where the vortex lattice in the ground state ($c=0$) is stable.

Since we are dealing with strong pinning, we expect that in the ground state the system of vortices "jumps" from one commensurate configuration with period ma to another when H is varied, with m large near H^N_{c1} and ending at $m=1$ near H^S_{c1} for $a \sim \lambda_S$. With further increase of field, the first-order commensurate structure $m=1$ breaks, and new incommensurate or higher-order commensurate structures are formed. The stability domain of the $m=1$ vs $m=2,3,\ldots$ commensurate structures can be determined by comparison of Gibbs free energies at a given T. Staying in the vicinity of a matching field, we have not attempted to determine the high-field end of the $m=1$ structure, which occurs when the energy of elastic deformation exceeds the pinning energy.

So far, we have considered the magnetic energy only. However, when c is of the order of the coherence length, the core of the vortex passes through a region where $g(x)\neq 1$, so along with the magnetic interaction, the core interaction must be taken into account. For $a_N \ll a$, as assumed before, the core energy density E^c can be calculated by multiplying the core energy (per unit vortex length) of an isolated vortex[15] by the number of vortices per unit area $n_v=1/aL$. Using the same reduced units as for the magnetic energy, we get

$$\tilde{E}^c=\frac{1}{8a\kappa_S L}\int_{-\pi/2}^{\pi/2}du\left[g^4(x)X_1(x)\cos u+\frac{3g^2(x)}{4}\cos^3 u\right], \tag{14}$$

where $x=(\sqrt{2}/\kappa_S)\tan u$, $X_1(x)=1$, for $|x-c|>a_N$, and $X_1(x)=0$ for $|x-c|<a_N$. Note that it is assumed here that $\kappa_N=0$ and $\xi_v=\sqrt{2}/\kappa_S$.[15] Numerical calculations done for several examples show that in each case the core pinning-force density

$$\tilde{f}^c=\frac{\partial \tilde{E}^c}{\partial c} \tag{15}$$

is an order of magnitude smaller than the magnetic force density $\tilde{f}^m$, so that the total pinning-force density is maximized at nearly the same point $c=c^*$ as determined from Eq. (13), and the critical configuration is almost unchanged.

In the critical state, we determine the critical-current density of the supercurrent flowing along the y axis from the force-balance equation.[19] In physical units,

$$j_{\rm cr}=\frac{cf_{\max}}{B}, \tag{16}$$

where $f_{\max}=f^m_{\max}+f^c_{\max}$ is the maximum of the total pinning-force density. Since in commensurate configurations all pinning centers act simultaneously,[1,10]

$$f=\frac{B}{\phi_0}f_1, \tag{17}$$

where f_1 is the pinning force per unit vortex length, and thus

$$j_{\rm cr}=\frac{c(f_1)_{\max}}{\phi_0}. \tag{18}$$

In reduced units,

$$\tilde{f}_1=aL(c^*)\tilde{f} \tag{19}$$

since $B=2\pi/[\kappa_S aL(c^*)]$, and

$$\tilde{j}_{\rm cr}=\frac{\kappa_S}{4\pi}\frac{j_{\rm cr}\lambda_S}{c\sqrt{2}H_c^S}=\frac{\kappa_S}{2\pi}aL(c^*)\tilde{f}_{\max}. \tag{20}$$

III. RESULTS AND DISCUSSION

The pinning force depends on two kinds of parameters: intrinsic (e.g., the thickness of the layers a_N, $a_S=a-a_N$, the coherence lengths $\xi_N(T_c),\xi_S(0)$, and the Ginzburg-Landau parameter κ_S) and extrinsic (e.g., temperature and external magnetic field). Taking $\xi_N(T_c)=\xi_S(0)$, we illustrate our results on the example $a/\lambda_S(0)=2$ and $\kappa_S=100$. We are then left with one intrinsic parameter, $a_N/\xi_N(T_c)$, where T_c is the transition temperature of the superlattice.

Note that the temperature dependence enters via $\lambda_S(t)$ and $H_c^S(t)$, where $t=T/T_c$ is the reduced temperature, and via the temperature dependence of the coherence length in the N phase in the dirty limit $\xi_N^2(T)=\xi_N^2(T_c)T_c/T$. Since $\lambda_S(t)=\lambda_S(0)/\sqrt{1-t}$ it follows that the period of the superlattice in reduced units is temperature dependent, $a(t)=[a/\lambda_S(0)]\sqrt{1-t}$. The thickness and the coherence length of the N layers, in reduced units, have the temperature dependences

$$\xi_N(t)=[\xi_N(t_c)/\lambda_S(0)]\sqrt{(1-t)/t}$$

and

$$a_N(t)=[a_N/\lambda_S(0)]\sqrt{1-t},$$

respectively.

Strong magnetic pinning occurs when $a_N \gtrsim a_N^*$, where $a_N^*\sim(1/\kappa_S)\ln\kappa_S$.[15] On the other hand, the validity of our approximate calculation requires $a_N \ll a$. These conditions imply, for $\xi_N(T_c)=\xi_S(0)$ and $a/\lambda_S(0)=2$, that $a_N/\xi_N(T_c)\sim 10$. For fixed $a_N/\xi_N(T_c)$, the magnetic pinning strength Γ is an increasing function of temperature t. At fixed t, Γ increases with $a_N/\xi_N(T_c)$ (Fig. 2). The

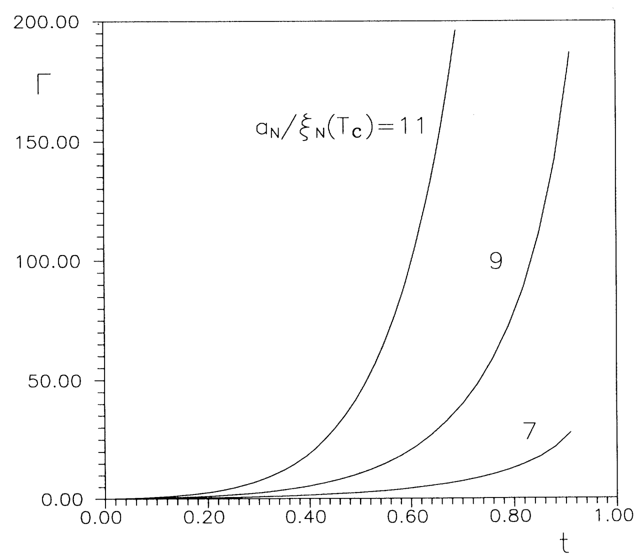

FIG. 2. Dependence of the pinning strength Γ on reduced temperature t for $a_N/\xi_N(T_c)=7$, 9, and 11, $\kappa_S=100$, and $a/\lambda_S(0)=2$.

above behavior can be understood analogously to the case of a single $S/N/S$ junction:[15] magnetic pinning is strong whenever the screening in N layers is weak. The order parameter g_N in N decreases with increasing t and/or $a_N/\xi_N(T_c)$: in both cases the screening weakens and Γ increases.

Next, we discuss the dependence of the pinning force and the critical current on $a_N/\xi_N(T_c)$ and t at a fixed value of the external field H, and on H for fixed values of the above parameters. In each case, before proceeding with the calculations we first verified that the $m=1$ configuration is the ground state of the vortex system throughout the entire parameter space. We present below an example of the procedure we used. To determine the ground state for $t=0.6$, $a_N/\xi_N(T_c)=7$, and $a/\lambda_S(0)=2$, we have considered a few competitive configurations of the vortices: when each N layer is occupied, every second, every third $(m=1,2,3,\ldots)$, etc.[2] For the corresponding pinning strength $\Gamma=4.42$, the diagrams of the Gibbs energy densities for $m=1$, 2, and 3 as functions of H are plotted in Fig. 3. In the field range just above H_{c1}^S, $0.028<H<0.08$, the configuration $m=1$ has the lowest energy. In the above field range, it is close to the hexagonal lattice, so considerable deformation is not needed to achieve the commensurability.

To compare the magnetic and core pinning, we plot on Fig. 4 the forces per unit vortex length $\tilde{f}_I^m$ and $\tilde{f}_1^c$, proportional to the corresponding parts of the critical-current density, as functions of $a_N/\xi_N(T_c)$ for $t=0.6$ and $H=0.036$. The core pinning force $\tilde{f}_1^c$ is calculated for the lattice displacement where it is the greatest. It turns out to be comparable to the critical displacement c^* for the magnetic pinning. The core pinning force saturates at $a_N/\xi_N\sim 1$, where the magnetic pinning force continues to increase, similarly to the case of a single vortex.[15] Note that the magnetic pinning is an order of magnitude greater than the core pinning.

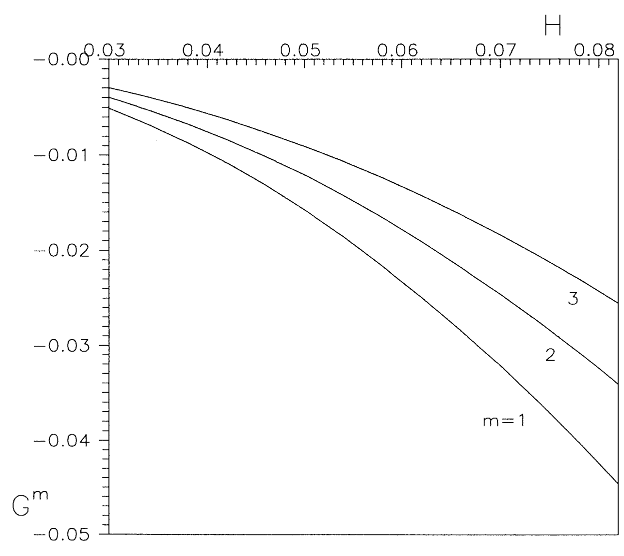

FIG. 3. Gibbs energy density $\tilde{G}^m$ vs external magnetic field H (in reduced units) for three configurations: $m=1,2,3$, for $t=0.6$, $a/\lambda_S(0)=2$, $\kappa_S=100$, and $a_N/\xi_N(T_c)=7$.

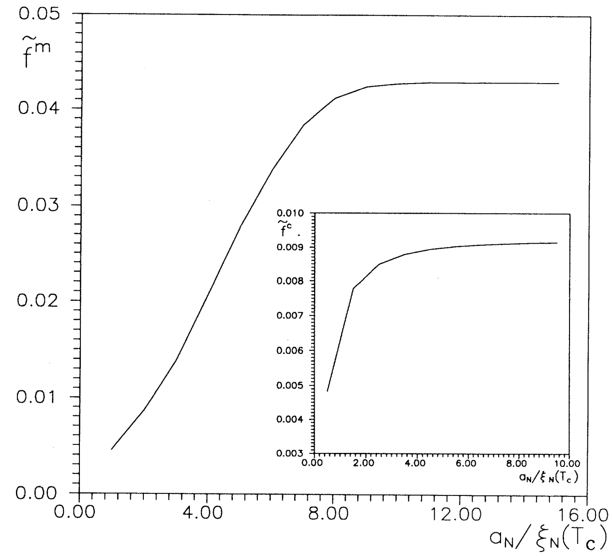

FIG. 4. Magnetic pinning force per unit vortex length $\tilde{f}_1^m$ vs the thickness of normal layer $a_N/\xi_N(T_c)$ for $\kappa_S=100$, $a/\lambda_S(0)=2$, $t=0.6$, and $H=0.036$. Inset: core pinning force per vortex $\tilde{f}_1^c$ vs the thickness of normal layer for the same set of parameters.

Our main results are nonmonotonic dependences of the critical-current density j_{cr} on temperature t (at fixed value of the external magnetic field H) and on H (at fixed t). There is a rapid increase (Fig. 5) of $\tilde{j}_{cr}$ with temperature from low t, where $a_N \ll \xi_N(t)$ and the supercurrent distribution is almost unperturbed, up to a maximum at $t=t^*$. This increase is due, as in the single-vortex case,[15] to the rapid increase of the magnetic pinning force with temperature. Above the optimum temperature t^* (for given H), there is a decrease until the pinning effects are washed out as $t\to t_c$.

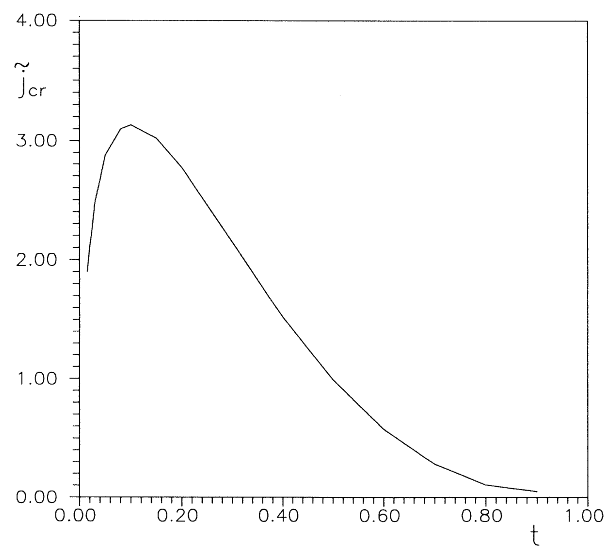

FIG. 5. Critical-current density $\tilde{j}_{cr}$ vs temperature t for $a/\lambda_S(0)=2$, $\kappa_S=100$, $a/\lambda_S(0)=2$, $a_N/\xi_N(T_c)=7$, and $H=0.04/(1-t)$.

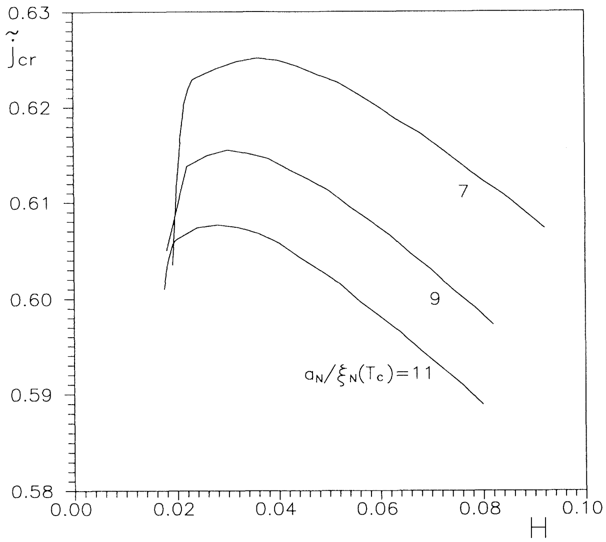

FIG. 6. Dependence of the critical-current density $\tilde{j}_{cr}$ on external magnetic field H for $t=0.6$, $a/\lambda_S(0)=2$, $\kappa=100$, and $\Gamma=4.42$, 20.82, and 98.09, which correspond to $a_N/\xi_N(T_c)=7$, 9, and 11.

The dependence of the $\tilde{j}_{cr}(H)$ on H is shown in Fig. 6 for $t=0.6$ and three different values of pinning strength Γ. In each case, the current density $\tilde{j}_{cr}(H)$ exhibits a maximum at $H=H_{max}$ in the vicinity of the matching field H_M corresponding to the matching induction $B_M=2\pi/(2\kappa_S a^2\sqrt{3})$: the vortex distances $L(H_{max})$ are in each case close to the matching distance $L_M=2a\sqrt{3}$. With increasing pinning strength, the peaks on the $\tilde{j}_{cr}(H)$ curves in Fig. 6 become higher and larger. In physical units, for typical values of the parameters $\xi_N(T_c)\sim\xi_S(0)\sim 10$ Å and $\kappa_s=100$, $j_{cr}(H_{max})$ is of the order of 10^7-10^8 A/cm^2.

IV. CONCLUSION

In this work we have investigated vortex pinning in HTC superconductor–normal-metal superlattices. We considered the main commensurate vortex configuration, $m=1$, in the range of the applied magnetic field where it is stable. For the case where the superlattice period a is comparable to λ_S, this range is close to H_{c1}^S. Pinning forces produced by such a superlattice in low fields can be very strong because in this region the effects of the magnetic pinning are most pronounced. In high applied field the overlapping of vortices smooths off the spatial variation of the local magnetic field, reducing the pinning effect. We note that in the present case of large κ the $m=1$ configuration stability domain cannot be extended to cover the whole range of the mixed state, from lower to upper critical field, as assumed in Ref. 20. This would require the superlattice period $a\sim\lambda$ near H_{c1}, where the distance between vortices is of the order of λ, and $a\sim\xi$ near H_{c2} where the vortex separation is comparable to ξ, which is possible only for κ of the order of unity.

Strong magnetic pinning of the vortex lattice is obtained when κ_S is large, $\xi_N(T_c)$ is small, and the temperature is not too low. In the critical state, rows of vortices are pinned in the vicinity of N/S interfaces, the critical displacement being $c^*\sim a_N/2\pm\xi_S$. A pronounced maximum of the critical current as a function of temperature is predicted. This effect, obtained also in the case of an isolated vortex,[15] is due to the rapid increase of the magnetic pinning with temperature. Experimentally, such behavior was observed[8] in PbIn/SnIn superlattices, and was explained by the transition of the weaker superconductor (Sn) in the normal state at a temperature near the maximum, $t\sim t^*$. In PbIn/Ag superlattices the maximum was not found.[21] However, in the latter systems,[8,21] with κ_S of the order of unity and ξ_N large, the pinning mechanisms (and their consequences) are different from those we considered. The important consequence of the increase of j_{cr} with temperature is the stabilization effect:[10] HTC superconductor–normal-metal superlattices are predicted to be more stable against flux jumps than conventional materials. The critical current has been shown to be nonmonotonic with applied field strength. This is a clear signature of the commensurability effect, since the maximum on the $j_{cr}(H)$ curve is in the vicinity of the corresponding matching field.[11–13] In our case, this maximum is situated in relatively low fields, in contrast to the usually observed peaks in high fields, due to the loss of vortex-lattice rigidity near the upper critical field.[10]

APPENDIX

In this Appendix, we calculate the free energy for a vortex lattice displaced a distance c from its equilibrium position. To solve Eq. (6), we take the local field to be periodic along the y direction,

$$h(x,y)=\frac{1}{L}\sum_{\forall l} e^{2\pi i l y/L} h_l(x) . \tag{A1}$$

Then Eq. (6) becomes

$$h_l(x)-\frac{d}{dx}\frac{1}{g^2}\frac{dh_l(x)}{dx}+\frac{1}{g^2}\frac{4\pi^2 l^2}{L^2}h_1(x) = \frac{2\pi}{\kappa_S}\sum_n \delta(x-na)e^{\pi i n l} , \tag{A2}$$

where we have used the Poisson formula to transform the right-hand side. By replacing x in Eq. (A2) with $x+a$, it can be shown that

$$h_l(x+a)=e^{\pi i l}h_l(x) . \tag{A3}$$

This means that it is necessary to solve Eq. (A2) only in the interval $[-a/2,a/2]$. In this region, Eq. (A2) becomes

$$Q^2 h_l(x)-\frac{d}{dx}\frac{1}{g^2}\frac{dh_l(x)}{dx} + \frac{4\pi^2 l^2}{L^2}\left[\frac{1}{g^2}-1\right]h_l(x)=\frac{2\pi}{\kappa_S}\delta(x) , \tag{A4}$$

where $Q^2=1+4\pi^2 l^2/L^2$. In the interior of the superconductor, $g(x)$ is nearly 1 $[g(x)-1\sim e^{-\kappa_S}]$ and Eq. (A4) becomes

$$Q^2 h_l - h_1'' = 0 \ . \tag{A5}$$

The solution is

$$h_l(x) = \begin{cases} A_l \cosh Qx + B_l \sinh Qx & \text{for } -a/2 < x < 0 \ , \\ C_l \cosh Qx + D_l \sinh Qx & \text{for } 0 < x < c \ , \\ x E_l \cosh Qx + F_l \sinh Qx & \text{for } c < x < a/2 \ . \end{cases} \tag{A6}$$

The coefficients A_l, B_l, C_l, D_l, E_l, and F_l can be determined from the boundary conditions at the N layer, and from the periodicity requirements, using Eq. (A3). Following Ref. 15, we integrate Eq. (A2) in the interval $(-M/2, M/2)$ to obtain the boundary condition for the derivative of $h_l(x)$. Since at the end of this interval h_l is asymptotically equal to the solution $h_l(x)$, and $h_l(0) = h_l(0)$, with accuracy $h_l(0)/\kappa_S$ when $a_N \sim 1/\kappa_S$, we get

$$-\left.\frac{dh_l(x)}{dx}\right|_{c-0}^{c+0} = \frac{4\pi^2 l^2}{L^2} \Gamma h_l(c) \ , \tag{A7a}$$

where Γ is given by Eq. (9). Thus

$$h_l(c-0) = h_l(c+0) \ . \tag{A7b}$$

The next boundary condition follows from symmetry under $x \to -x$,

$$h_l(-0) = h_l(+0) \ , \tag{A7c}$$

$$h_l'(-0) - h_l'(+0) = 2\pi\kappa_S \ , \tag{A7d}$$

and from Eq. (A3) we get

$$h_l\left[-\frac{a}{2}\right] = (-1)^l h_l\left[\frac{a}{2}\right] \ , \tag{A7e}$$

and

$$h_l'\left[-\frac{a}{2}\right] = (-1)^l h_l'\left[\frac{a}{2}\right] \ . \tag{A7f}$$

Using the above conditions we find the solution $h(x,y)$. This solution is the asymptotic limit of the exact solution of Eq. (A4) in the limit of large κ_S and small a_N/λ_S. Using this asymptotic limit and with the help of Eq. (7) we calculate the magnetic energy density, Eq. (8).

[1] M. Tachiki and S. Takahashi, Solid State Commun. **70**, 291 (1989).
[2] B. I. Ivlev and N. B. Kopnin, Phys. Rev. Lett. **64**, 1828 (1990).
[3] W. K. Kwok, U. Welp, V. M. Vinokur, S. Fleshler, J. Downey, and G. W. Crabtree, Phys. Rev. Lett. **67**, 390 (1991).
[4] R. A. Doyle, A. M. Campbell, and R. E. Somekh, Phys. Rev. Lett. **71**, 4241 (1993).
[5] P. Monceau, D. Saint James, and G. Waysand, Phys.Rev. B **12**, 3673 (1975).
[6] P. Martinoli, J. L. Olsen, and J. R. Clem, J. Less-Common Met. **62**, 315 (1978).
[7] H. Raffy, J. C. Renard, and E. Guyon, Solid State Commun. **11**, 1679 (1972); **14**, 427 (1974).
[8] H. Raffy, C. A. Acad. Sci. Ser. B **284**, 559 (1977).
[9] Y. Kuwasawa, T. Tosaka, A. Uchiyama, S. Matsuda, and S. Nakano, Physica C **175**, 1751 (1991).
[10] A. M. Campbell and J. M. Evetts, Adv. Phys. **21**, 199 (1972).
[11] Lj. Dobrosavljević, J. Phys. (Paris) **37**, 23 (1976).
[12] P. Martinoli, Phys. Rev. B **17**, 1175 (1978).
[13] S. Ami and K. Maki, Prog. Theor. Phys. **53**, 1 (1975).
[14] A. N. Lykov, Adv. Phys. **42**, 263 (1993).
[15] D. Davidović and L. Dobrosavljević-Grujić, Phys. Rev. B **43**, 2809 (1991).
[16] M. Tachiki, S. Takahashi, and K. Sunaga, Phys. Rev. B **47**, 6095 (1993).
[17] Lj. Dobrosavljević-Grujić, V. Prokić, and D. Davidović, in *Proceedings of SPIE OE/LASE '94, Superconducting Superlattices and Multilayers,* edited by I. Bozovic (SPIE, Bellingham, WA, 1994), p. 50.
[18] Orsay Group on Superconductivity, in *Quantum Fluids,* edited by D. F. Brewer (North-Holland, Amsterdam, 1966).
[19] P. G. de Gennes, Superconductivity (Benjamin, New York, 1966).
[20] S. Takahashi, T. Hirai, and M. Tachiki, in *Proceedings of SPIE OE/LASE '94, Superconducting Superlattices and Multilayers* (Ref. 17), p. 263.
[21] H. Raffy and E. Guyon, J. Phys. (Paris) Colloq. **39**, C6-646 (1978).